Photoacoustics 30 (2023) 100465

Contents lists available at ScienceDirect

Photoacoustics

journal homepage: www.elsevier.com/locate/pacs

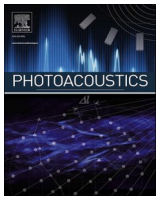

Ultrafast measurement of laser-induced shock waves

Žiga Lokar, Darja Horvat, Jaka Petelin, Rok Petkovšek *

University of Ljubljana, Faculty of Mechanical Engineering, Aškerčeva 6, 1000 Ljubljana, Slovenia

ARTICLE INFO

Keywords:
Laser-induced shockwave
Shockwave rise time
Fiber optic hydrophone
Viscosity

ABSTRACT

We present measurements of laser-induced shockwave pressure rise time in liquids on a sub-nanosecond scale, using custom-designed single-mode fiber optic hydrophone. The measurements are aimed at the study of the shockwave generation process, helping to improve the effectiveness of various applications and decrease possible accidental damage from shockwaves. The developed method allows measurement of the fast shockwave rise time as close as 10 μm from an 8 μm sized laser-induced plasma shockwave source, significantly improving the spatial and temporal resolution of the pressure measurement over other types of hydrophones. The spatial and temporal limitations of the presented hydrophone measurements are investigated theoretically, with actual experimental results agreeing well with the predictions. To demonstrate the capabilities of the fast sensor, we were able to show that the shockwave rise time is linked to liquid viscosity exhibiting logarithmic dependency in the low viscosity regime (from 0.4 cSt to 50 cSt). Additionally, the shockwave rise time dependency on propagation distance close to the source in water was investigated, with shock wave rise times measured down to only 150 ps. It was found that at short propagation distances in water halving the shock wave peak pressure results in the rise time increase by approximately factor of 1.6. These results extend the understanding of shockwave behavior in low viscosity liquids.

1. Introduction

With the emergence of numerous new technologies and procedures in the field of laser-assisted medicine and other technological advances in the aqueous environment, weak and strong shockwaves are created in a variety of industrial or medical processes, either on purpose or as an undesired side effect. The need for detection and monitoring of these phenomena is also rapidly increasing. Many of the new technologies tend towards miniaturization, inevitably involving very high-speed events. The rapidly growing use of lasers in medicine requires characterization of many different phenomena that occur in tissue and aqueous environments, often following the formation of micro- and nanobubbles which are generated intentionally or unintentionally during therapeutic and diagnostic procedures. The formation of a laser-induced bubble is accompanied by a shock wave creation [1], for example during laser surgery and eye therapies, such as capsulotomy, refractive surgery (vision correction), vitreolysis, selective retina therapy [2] or during the formation of laser-induced plasmonic vapor nanobubbles in various fields, from biophotonics and medicine [3], such as cancer therapy [4] and photoacoustic imaging, to surface cleaning, study of cavitation erosion [5] and emerging and expanding solar energy harvesting technology [6]. Nanoplasmonics promises the use of nanoscale vapor bubbles for diagnostic and therapeutic purposes on sub-cellular and even molecular structures with extremely high precision [7]. Efforts are made towards miniaturization, possibly leading to the possibility of manipulating small biological objects down to cell scale [8]. The existence of sharp pressure gradients is characteristic of shock wave generation and propagation, so reliable measurement of pressure rise time is of crucial importance.

In medical therapy and diagnostics, the safety of a procedure is a constant concern. The question as to what is the primary cause of laser-induced mechanical damage in the case of a single cell is still not completely resolved: is it the rapidly growing laser-induced cavitation bubble or the shock wave released as the bubble expands, the latter with two possible contributing reasons: the large peak pressure and the large spatial and temporal pressure gradients, owing to the fast rise time [9,10]. The answer depends largely on the individual circumstances of each application [11,12]. While investigating the origin of laser-induced retina pigment epithelium damage Brinkmann et al. [13] already mentioned that stress gradient is possibly more important regarding the cell damage than the peak stress itself but concluded that the complexity of the system did not allow to determine with certainty what is the main

* Corresponding author.
E-mail address: rok.petkovsek@fs.uni-lj.si (R. Petkovšek).

https://doi.org/10.1016/j.pacs.2023.100465
Received 21 September 2022; Received in revised form 1 February 2023; Accepted 21 February 2023
Available online 23 February 2023

contributing factor to the cell damage. The importance of the stress rise time was recognized also by Doukas et al. [14] when they showed that the cellular damage by stress waves correlates better with the stress rise time than by its peak value while Douki et al. [15] observed lower cell killing for 20 ns rise time pulses than for 10 ns rise times. In a study by Lombard et al. [9] critical pressure rise time was found to be 5 MPa/ns, at least for lower power energy input as is pursued in medical use of lasers today.

In the works [16,17] the possibility is shown to experimentally determine viscosity by measurement of pressure and rise time in the liquid. Their work was performed in solids and highly viscous glycerol, while we extend their analysis by measurements of rise time in lower viscosity liquids. These liquids are expected to exhibit much shorter rise times, therefore a very fast detector is required. Additionally, aforementioned pursuit of miniaturization led us to measure very close to the breakdown site, at distances even below 20 μm. Fortunately, the small size of the detector is associated with high bandwidth and short events, enabling both miniaturization and speed with the same sensor.

This work describes the measurement results of a custom-built miniature fiber optic pressure hydrophone (FOPH) used in a custom-built experimental system. Sensor limitations are analysed theoretically and experimentally. Capabilities of both localized and fast measurement are demonstrated by very fast pressure measurements in close proximity to the shockwave generating laser-induced plasma. Finally, further improvements are discussed.

2. Methods

2.1. Experimental setup

A 60 ps pulse from laser (single pulse operation mode) with 1030 nm wavelength for this experiment is focused through a 40 × high numerical aperture (NA) microscope objective to produce dielectric breakdown in water and other liquids. NA of the setup is 0.5 for breakdown imaging in water. The laser produced 1.5−7.5 μJ pulses. The breakdown threshold was approximately 1 μJ.

Fiber optic probe hydrophone was used to measure the shockwave pressure. It is based on a single-mode fiber with 5/125 μm core/cladding diameter and 6.6 μm mode field diameter (MFD). The latter number defines the sensing element size and the resulting capabilities. A 1030 nm wavelength, single mode laser light source was used. The hydrophone was fixed inside a liquid container in the direction perpendicular to the incident laser beam and moved in 3D together with the container to scan the pressure waveforms at different distances from the breakdown (Fig. 1).

The fiber optic hydrophone used in this study works by measuring the change of light reflectance at the fiber tip [18,19]. In unperturbed water, the reflectance occurs between the media with refractive indices 1.45 (glass) and 1.3246 (water), respectively; resulting in 0.204% reflection. The reflected light is guided to a 5 GHz photodiode, the output of which is recorded by a 12 GHz oscilloscope. In the used setup, the detection bandwidth is limited primarily by the photodiode characteristic. The shockwave compression leads to water refractive index increase and in turn a change in the reflectance at the hydrophone tip, changing the amount of light incident on the photodiode. To obtain the pressure from the raw voltage data, produced by the photodiode and recorded by the oscilloscope, first the refractive index corresponding to each data point in the oscilloscope trace was calculated from reflectance. The water density change with pressure [20] and the refractive index dependence on density [21] were used to calculate the pressure. The fact that the incident and the reflected acoustic wave pressures both contribute to the refractive index change at the liquid-glass interface was also accounted for. The sensitivity of the hydrophone is approximately 2 mV/MPa.

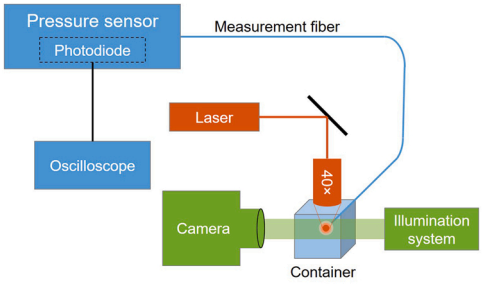

Fig. 1. Experimental setup. Pressure sensor detects shockwaves generated in liquid by a laser pulse, focused through a high-NA microscope objective. Camera and illumination laser are used to image the generated breakdown and related phenomena.

The 3D printed container is covered by a microscope cover glass (18 ×18 ×0.15 mm). Two of the container side walls are also built of such cover slides and are used as windows for the camera and the laser illumination [22]. Perpendicular to both the camera and the laser, a small hole for hydrophone insertion is made in a side wall of the container. The fiber is inserted through the hole and fixed, allowing it to move together with the container. The container is positioned on a 3D translation stage, while the path of the laser beam is fixed. This enables pressure data acquisition at different locations with respect to the breakdown site. Several liquids were used and every liquid was placed in a separate container to avoid contamination. The tip of the fiber was freshly cleaved and cleaned before performing measurements in different liquids, which were, in order of increasing viscosity: acetone ($\eta = 0.38$ cSt), water (R>1 MΩ, $\eta = 0.89$ cSt), isopropyl alcohol (IPA, $\eta = 2.5$ cSt), silicone oil ($\eta = 5$ cSt) and silicone oil ($\eta = 50$ cSt). Viscosities are given at 25 °C, which was the temperature of the room and liquid in all cases. The heating by the hydrophone is negligible, the temperature increase is calculated to be under 0.1 °C in water. The breakdown produces a large temperature increase at the focusing spot locally, generating plasma. However, the average temperature increase in the sphere with radius of 100 μm is below 1 °C. This contribution to the increased liquid temperature (and in turn changed liquid parameters) was also ignored.

All of the liquids used have lower refractive indices than glass, therefore the same procedure was used to convert the voltage to pressure as explained previously for water. However, due to insufficient data on the detailed refractive index change with pressure, only the normalized pressure is shown for other liquids, assuming the trends are the same as for water.

2.2. Consideration of sensor limitations due to geometry

The main reason for choosing the single-mode fiber over the multimode is the size of the active area (fiber core) which is much smaller in the case of a single-mode fiber (5 μm), enabling spatially and temporally very local measurements [23]. However, there is still some broadening of the measured signal, the main contributing factor being due to geometry: the fact that both, the sensing element of the hydrophone as well as the shock wave source are not points but each of them has a finite dimension. The effects are analyzed in Fig. 2.

The mechanism through which the lateral spatial dimension of the hydrophone tip sensing area causes the broadening of the measured signal are the different times that the curved shock wavefront takes to travel to different parts of the sensing area. The time difference Δt between the first and the last arrival of different parts of a single wavefront to the sensing area is plotted in Fig. 2a for different fiber positioning angles ϕ, where $\phi = 0°$ denotes the configuration when the normal to the fiber end face is parallel to the line connecting the shock source and the sensor. Distance d and angle ϕ are sufficient to characterize the fiber position with respect to the source since any transversal offset can be converted to a new (slightly larger) distance between the source and the fiber center and a new fiber positioning angle. This relation is explained

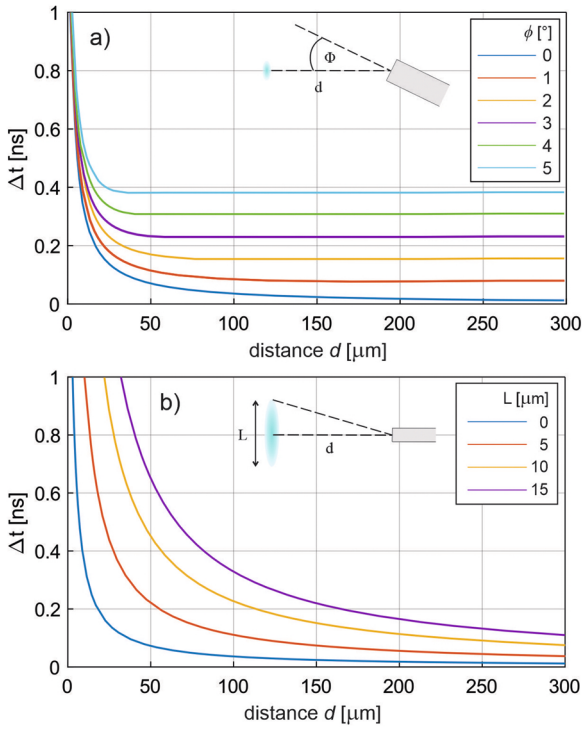

Fig. 2. Broadening of the measured pressure signal due to geometrical reasons: fiber positioning (a) and plasma length L (b).

in more detail in [23], together with the analysis of frequency response which is not repeated, as it was shown there that it only plays a role on longer time scales, which are not of interest here.

The second contribution to the signal broadening is due to the finite dimension of the shock wave source. In the above analysis of broadening due to hydrophone positioning the shockwave is assumed to originate from a point source and propagate spherically; in reality the source has a finite dimension which further increases Δt, as shown in Fig. 2(b) for four different source dimensions close to the one used in our experiments. The length of the source L refers to the length of the source as seen from the fiber – the projection of the source to the plane defined by the fiber end face. Other dimensions of the source are not considered, since the analysis is only an estimation of the signal broadening effects and is not an attempt to calculate exact contributions or sensor response. In this light it needs to be pointed out that the calculated Δt is actually an over-estimate of the effective signal broadening, as the weighted contributions at the beginning and the end of the shockwave-hydrophone interaction to the measured signal are considerably smaller than the contribution of the central portion. Additionally, to compensate for the noise of the measurement system, in the analysis of rise times presented in continuation the time taken for pressure to grow from 10% to 90% or 20–80% was considered to be the rise time, as it is also customary in such analyses.

A camera at high magnification (2 μm per pixel) was used for precise fiber positioning as well as to measure the plasma size. We estimate that the fiber was aligned well within 5° for all measurements except possibly the closest few. The plasma width representing the shockwave source dimension is assessed to be approximately 8 μm.

The acoustic reflection ratio at the liquid-glass boundary was calculated from the acoustic impedances of unperturbed liquid and unperturbed quartz, presented in Table 1.

Acoustic impedance was calculated from speed of sound in liquid and density data. For both silicon oils, shockwave velocity was first measured using two illumination pulses in a single camera frame to image the shockwave propagation, using the imaging setup described in [22].

Table 1
Acoustic impedance and reflection.

Material	Quartz	Water	Acetone	IPA	Oil, 5 cst	Oil,50 cst
Acoustic impedance [MPa·s/m]	12.1	1.5	0.92	0.95	0,89	0,97
Reflection on quartz	/	63%	74%	73%	75%	73%

The table was used to calculate the unperturbed pressure in other liquids besides water; however, the relative refractive index change with pressure was assumed to be the same as for water. As the validity of this assumption may be poor, we opted to show only the normalized pressure for other liquids.

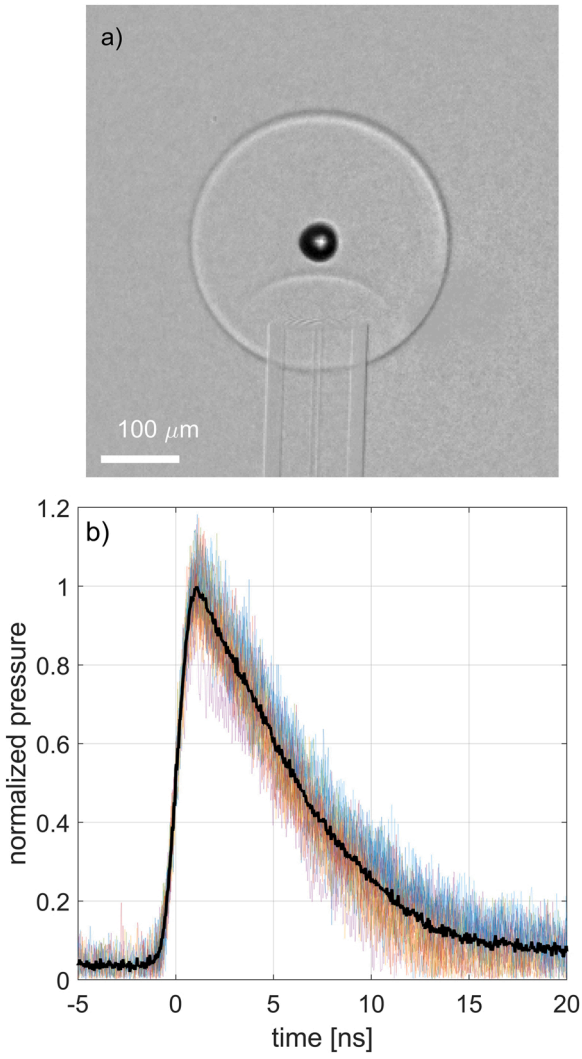

Fig. 3. A typical pressure measurement configuration close to the breakdown (a). The image shows the fiber pressure sensor (hydrophone) with the bubble growing at the breakdown site and the spherically propagating shockwave. Laser is incident from the right. Plasma is visible in the center of the bubble. The sensing element of the fiber (5 μm diameter) can be distinguished from the fiber cladding (125 μm diameter). The part of the shockwave that was reflected from the fiber tip can be observed propagating in the opposite direction, approaching the bubble. The pressure trace (b, black curve) shows the average of 30 measurements (shown in different colors). All traces are scaled relative to the normalized maximum pressure of 1 for the average trace.

3. Results and discussion

The image of the breakdown site, primarily used for fiber positioning, is presented in Fig. 3a. Laser pulse with 2.5 μJ energy is incident from the right. The bubble following the laser induced breakdown plasma can be observed, as well as the spherically propagating shockwave. The reflected shockwave from the fiber tip is seen to preserve its phase upon reflection, as expected, and appears to have a smaller amplitude. The fiber-breakdown distance is assessed to be 105 μm.

Apart from the noise, the 30 individual pressure measurements, presented in Fig. 3b, are comparable in shape and amplitude. The black curve is the average of the 30 waveforms, eliminating the noise to a great extent. The measurement was performed in isopropyl alcohol (IPA). Full-width-half-maximum (FWHM) of the average pressure waveform is 6 ns, while the pressure rise time, measured between 20% and 80% of the peak pressure is 530 ps for this measurement.

Shock wave pressure transients detected in various liquids with different viscosities at approximately the same distance of 100 μm are presented in Fig. 4(a) together with the results of the rise time dependence on liquid viscosity (Fig. 4b).

In accordance with reports from other researchers [16,17,24] and theory [25], the shockwave rise time is related to viscosity, where lower viscosity liquids exhibit sharper rise times. Other groups show different trends for rise time change with viscosity and pressure for various solid materials [17] and glycerol [16]. In our case of up to three orders of magnitude lower viscosity than previously reported, there is evidence that the trend is similar.

Both the 10–90% as well as the 20–80% rise times, measured at the same distance from the source, are shown to increase with increasing viscosity. This trend holds from acetone with low viscosity of 0.38 cSt to silicon oil with viscosity of 50 cSt. There is little difference in trends of 10–90% rise time and 20–80% rise time, except for the very viscous 50 cSt silicon oil, which exhibits issues with noise despite averaging. The trend appears approximately linear on a semi-logarithmic scale, implying logarithmic dependence of rise time on viscosity, $rt \propto \ln(\eta)$. The observed increase of shock wave rise time with viscosity is consistent with the experimental findings on effects of viscosity on laser-induced shock dynamics by others [26,27].

The strain rate which is roughly proportional to the inverse of the shock wave rise time, is found [16] to be proportional to shear stress and inversely proportional to viscosity in the first approximation. We have observed slower than linear increase of rise time with viscosity in our measurements, especially for the 50 cSt oil, having largest viscosity. However, the shear stress was not measured which may contribute to the discrepancy. Rise time may be underestimated for the 50 cSt oil due to smaller shock wave width, presumably caused by relatively more energy dissipation and cutting off the peak of the shock wave pressure.

Additional rise time analysis was performed in water. Using NIR laser pulses at different energies, we analysed the rise time with distance from breakdown (Fig. 5). The data points correspond to 20–80% rise time.

The measurements exhibit lower shockwave rise times very close to the source (less than 50 μm), reproducible over many different distances and at different laser pulse energies. This rapid increase of the measured rise time close to the source can be explained by the above analysis illustrated in Fig. 2 – both contributions to the sensor response broadening rise sharply in this region. The calculated Δt for the same distance range and 8 μm measured plasma diameter was multiplied by 0.6 to account for the comparison with the 20–80% rise time rather than the full value. For the assumed perfect fiber positioning the sensor limit matches the observed rise times very well. Therefore, to improve on measurement results at short distances, it would be required to either reduce the plasma size or use an optical fiber with even smaller mode field diameter. At distances of approximately 100 μm we obtain the shortest rise times of 150 ps, while at longer distances the rise time starts increasing. The increase of rise time at larger distances from the source is not brought on by a measurement limitation. Here, the cause is the shockwave peak pressure decreasing with distance, which in turn broadens the shock wave profile, increasing the rise time. The peak pressure decrease with distance is shown in Fig. 6, while the rise time changes with pressure are analysed in Fig. 7.

The peak pressure is found to decrease with distance with power law,

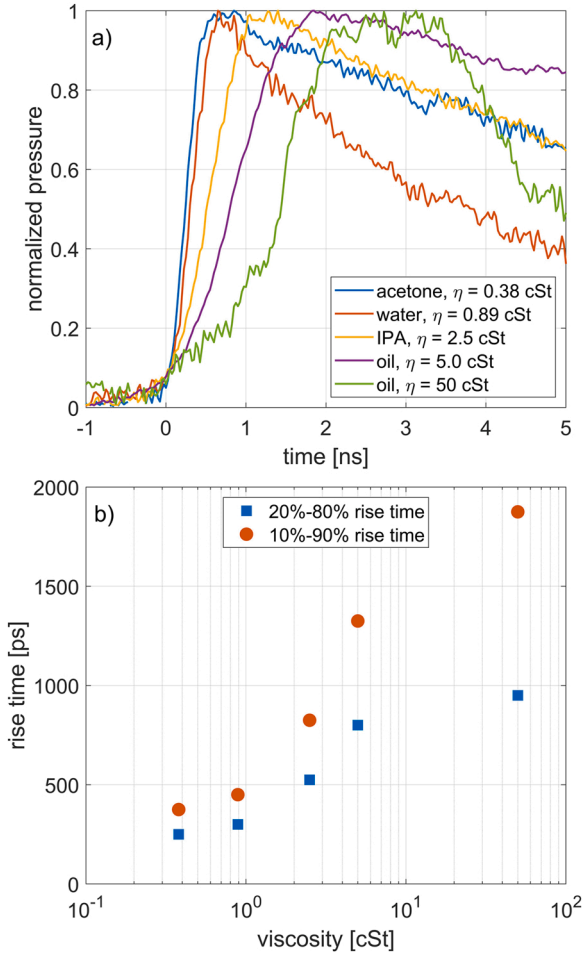

Fig. 4. Normalized pressure traces (a) and corresponding rise times (b) for different liquids. In liquids with lower viscosity the shockwaves are sharper.

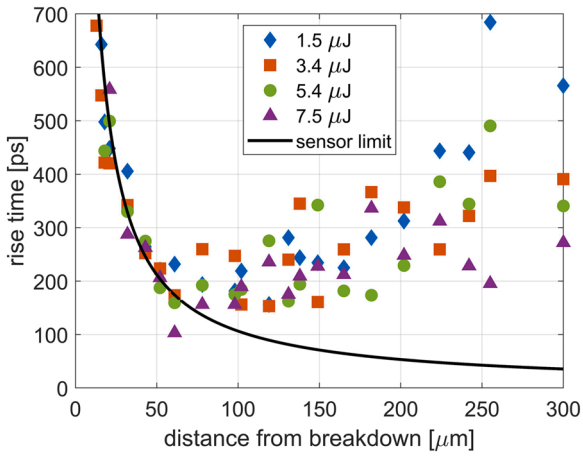

Fig. 5. Rise time as a function of distance from the source and laser energy. Shortest rise times are observed for distances of approximately 100 μm, while both at shorter and at longer distances the measured rise time is larger. The black curve is the sensor geometrical limitation for an 8 μm wide source (see text for detailed explanation).

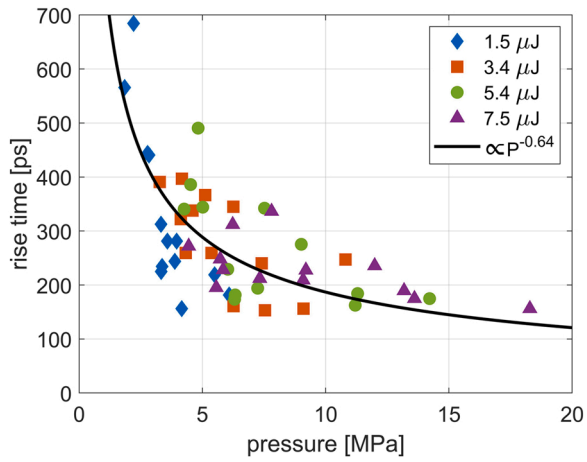

Fig. 6. Pressure decrease with distance. Decay follows d^{-x} trends, with different x depending on pulse energy.

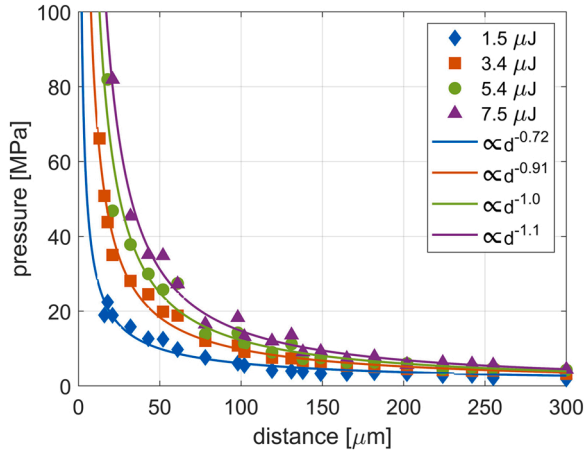

Fig. 7. Rise time decreases with increasing pressure. Data points before 100 μm distance are not shown.

the exponent depending on the experimental circumstances [27–29], such as breakdown energy or shape and propagation geometry (spherical, cylindrical or a combination) and the shock wave decay. Here function ad^{-b} was fitted to shock waveforms at various laser pulse energies. The fits follow experimental values well, with only a few data points above or below the trendline. The value of the exponent b increases with laser pulse energy. As the plasma appears to be nearly spherical at all laser energies, we believe that the dominant reason is that the shock wave decays proportional to d^{-2}, while an acoustic wave decays with d^{-1} [30]. Therefore, at higher initial energies the shockwave pressure decay is faster, as was also noted by [27,29]. However, while other groups have measured or calculated faster decay than d^{-1} in spherical geometry we have also observed slower decays for lower energy pulses. This suggests that in our experiment at such short distances we are still observing the formation of the shockwave as opposed to a fully developed shockwave farther away from the source.

Despite the variation in rise time, the observed trend is that increasing peak pressure leads to decreased rise time (Fig. 7). Data points in the region where they are clearly limited by the sensor characteristics – closer than 100 μm – are excluded from this analysis. For the lowest energy, rise time decreases slightly faster and reaches very low values even at pressure of around 5 MPa; this might be an indicator of a more spherical plasma than in the case of higher energies, consistent with the observations in Fig. 6. Even though different energies lead to slightly different plasma sizes and shapes, these differences are negligible for distances from 100 μm onward. Fitting of the power law on the data (ax^{-b}, the same as in case of pressure decay with distance) yields rise time dependence on pressure as $rt \propto P^{-0.64}$. In comparison, [24] observed strain rate dependence on pressure to be $\dot{\epsilon} \propto P^{2.1}$ in glycerol, while [17] measured the exponent to be close to 4 in solids. Therefore, our results suggest that for lower viscosities like that of water, the rise time decrease with increasing pressure is slower than for higher viscosity liquids like glycerol and for solids. At higher pressures, even shorter rise times than the ones obtained here would be expected. Unfortunately, the data points associated with peak pressures beyond 20 MPa correspond to the pressure sensor very close to the source, meaning the geometrical limitations of the setup are reached and exceeded, while increasing the pulse energy further was not an option using this laser.

4. Conclusion

The picosecond laser-induced shock wave transient pressure was measured very close to the plasma source by a custom-made single mode fiber hydrophone, offering (to our knowledge) unmatched spatial and temporal resolution of pressure measurement in comparable circumstances. The analysis of the hydrophone limitations reveal that the hydrophone response broadening is governed by the fiber alignment and, as we approach the source, by the source dimensions. When the source size and distance from the sensor are comparable to the hydrophone active area (6.6 μm) the spatial and temporal resolution become affected.

With the described limitations we were able to measure shock wave rise times down to 150 ps. Measurements in various liquids revealed that the rise time increases with approximately logarithm of viscosity, in the relatively low viscosity regime from 0.4 cSt to 50 cSt.

Measurement of shock wave rise time dependency on the distance was performed in water. As the shockwave propagates and dissipates energy, increased rise time is measured. Halving the peak pressure was observed to increase the rise time by a factor of approximately 1.6.

Finally, having a shock wave source with very small dimensions (down to 8 μm) at very close distances of below 20 μm, we have clearly reached the spatial limitation of our 6.6 μm active diameter sensor, as can be seen from the shockwave rise times at close distance that are evidently limited by the measurement setup. To measure even faster rise times even closer to a more localized laser induced breakdown, an even smaller sensing element is required.

Funding

This work was funded by the Slovenian Research Agency (research core funding No. P2-0270 and project Nos. L2-3171 and J2-3057).

Declaration of Competing Interest

The authors declare that they have no known competing financial interests or personal relationships that could have appeared to influence the work reported in this paper.

Data availability

Data will be made available on request.

References

[1] A. Vogel, S. Busch, U. Parlitz, Shock wave emission and cavitation bubble generation by picosecond and nanosecond optical breakdown in water, J. Acoust. Soc. Am. 100 (1996) 148–165.

[2] E. Seifert, J. Tode, A. Pielen, D. Theisen-Kunde, C. Framme, J. Roider, Y. Miura, R. Birngruber, R. Brinkmann, Algorithms for optoacoustically controlled selective retina therapy (SRT), Photoacoustics 25 (2022), 100316, https://doi.org/10.1016/j.pacs.2021.100316.

[3] A.M. Fales, W.C. Vogt, K.A. Wear, T.J. Pfefer, I.K. Ilev, Experimental investigation of parameters influencing plasmonic nanoparticle-mediated bubble generation with nanosecond laser pulses, JBO 24 (2019), 065003, https://doi.org/10.1117/1.JBO.24.6.065003.
[4] X. Huang, P.K. Jain, I.H. El-Sayed, M.A. El-Sayed, Plasmonic photothermal therapy (PPTT) using gold nanoparticles, Lasers Med. Sci. 23 (2008) 217–228, https://doi.org/10.1007/s10103-007-0470-x.
[5] F. Reuter, C. Deiter, C.-D. Ohl, Cavitation erosion by shockwave self-focusing of a single bubble, Ultrason. Sonochem. (2022), 106131, https://doi.org/10.1016/j.ultsonch.2022.106131.
[6] G. Baffou, F. Cichos, R. Quidant, Applications and challenges of thermoplasmonics, Nat. Mater. 19 (2020) 946–958, https://doi.org/10.1038/s41563-020-0740-6.
[7] E. Boulais, R. Lachaine, A. Hatef, M. Meunier, Plasmonics for pulsed-laser cell nanosurgery: Fundamentals and applications, J. Photochem. Photobiol. C Photochem. Rev. 17 (2013) 26–49, https://doi.org/10.1016/j.jphotochemrev.2013.06.001.
[8] X. Yan, G.J. Diebold, Generation of high amplitude compressions and rarefactions in a photoacoustically excited droplet, Photoacoustics 23 (2021), 100289, https://doi.org/10.1016/j.pacs.2021.100289.
[9] J. Lombard, J. Lam, F. Detcheverry, T. Biben, S. Merabia, Strong and fast rising pressure waves emitted by plasmonic vapor nanobubbles, Phys. Rev. Res. 3 (2021), 023231, https://doi.org/10.1103/PhysRevResearch.3.023231.
[10] S.A. Hussain, C. Milián, C. Crotti, L. Kowalczuk, F. Alahyane, Z. Essaïdi, A. Couairon, M.-C. Schanne-Klein, K. Plamann, Cell viability and shock wave amplitudes in the endothelium of porcine cornea exposed to ultrashort laser pulses, Graefes Arch. Clin. Exp. Ophthalmol. 255 (2017) 945–953, https://doi.org/10.1007/s00417-017-3583-3.
[11] J.H. Song, A. Moldovan, P. Prentice, Non-linear acoustic emissions from therapeutically driven contrast agent microbubbles, Ultrasound Med. Biol. 45 (2019) 2188–2204, https://doi.org/10.1016/j.ultrasmedbio.2019.04.005.
[12] A.G. Doukas, T.J. Flotte, Physical characteristics and biological effects of laser-induced stress waves, Ultrasound Med. Biol. 22 (1996) 151–164, https://doi.org/10.1016/0301-5629(95)02026-8.
[13] R. Brinkmann, G. Hüttmann, J. Rögener, J. Roider, R. Birngruber, C.P. Lin, Origin of retinal pigment epithelium cell damage by pulsed laser irradiance in the nanosecond to microsecond time regimen, Lasers Surg. Med 27 (2000) 451–464, https://doi.org/10.1002/1096-9101(2000)27:5<451::AID-LSM1006>3.0.CO;2-1.
[14] A.G. Doukas, D.J. McAuliffe, S. Lee, V. Venugopalan, T.J. Flotte, Physical factors involved in stress-wave-induced cell injury: the effect of stress gradient, Ultrasound Med. Biol. 21 (1995) 961–967, https://doi.org/10.1016/0301-5629(95)00027-O.
[15] T. Douki, S. Lee, K. Dorey, T.J. Flotte, T.F. Deutsch, A.G. Doukas, Stress-wave-induced injury to retinal pigment epithelium cells in vitro, Lasers Surg. Med. 19 (1996) 249–259, https://doi.org/10.1002/(SICI)1096-9101(1996)19:3<249::AID-LSM1>3.0.CO;2-S.
[16] G.I. Kanel, A.S. Savinykh, G.V. Garkushin, S.V. Razorenov, Evaluation of glycerol viscosity through the width of a weak shock wave, High Temp. 55 (2017) 365–369, https://doi.org/10.1134/S0018151×17030105.
[17] J.W. Swegle, D.E. Grady, Shock viscosity and the prediction of shock wave rise times, J. Appl. Phys. 58 (1985) 692–701, https://doi.org/10.1063/1.336184.
[18] J. Staudenraus, W. Eisenmenger, Fibre-optic probe hydrophone for ultrasonic and shock-wave measurements in water, Ultrasonics 31 (1993) 267–273, https://doi.org/10.1016/0041-624X(93)90020-Z.
[19] G. Sinibaldi, A. Occhicone, F. Alves Pereira, D. Caprini, L. Marino, F. Michelotti, C. M. Casciola, Laser induced cavitation: plasma generation and breakdown shockwave, Phys. Fluids 31 (2019), 103302, https://doi.org/10.1063/1.5119794.
[20] E.W. Lemmon, I.H. Bell, M.L. Huber, M.O. McLinden, Thermophysical Properties of Fluid Systems, NIST Standard Reference Database Number 69, National Institute of Standards and Technology, Gaithersburg MD, 20899, USA, n.d. ⟨https://doi.org/10.18434/T4D303⟩, (Accessed 12 July 2022).
[21] I. Thormählen, J. Straub, U. Grigull, Refractive index of water and its dependence on wavelength, temperature, and density, J. Phys. Chem. Ref. Data 14 (1985) 933–945, https://doi.org/10.1063/1.555743.
[22] V. Agrež, T. Požar, R. Petkovšek, High-speed photography of shock waves with an adaptive illumination, Opt. Lett. 45 (2020) 1547–1550, https://doi.org/10.1364/OL.388444.
[23] J. Petelin, Z. Lokar, D. Horvat, R. Petkovsek, Localized measurement of a sub-nanosecond shockwave pressure rise time, IEEE Trans. Ultrason. Ferroelectr. Freq. Control 69 (2022) 369–376, https://doi.org/10.1109/TUFFC.2021.3115629.
[24] G.I. Kanel, A.S. Savinykh, G.V. Garkushin, A.V. Pavlenko, S.V. Razorenov, Shock wave rise time and the viscosity of liquids and solids, in: H. Altenbach, R. V. Goldstein, E. Murashkin (Eds.), Mechanics for Materials and Technologies, Springer International Publishing, Cham, 2017, pp. 257–263, https://doi.org/10.1007/978-3-319-56050-2_13.
[25] I.B. Zel′dovich, I.P. Raĭzer, Physics of Shock Waves and High-temperature Hydrodynamic Phenomena, Dover Publications, Mineola, N.Y, 2002.
[26] H. Kurahara, K. Ando, Effects of liquid viscosity on laser-induced shock dynamics. Volume 5: Multiphase Flow, American Society of Mechanical Engineers, San Francisco, California, USA, 2019, https://doi.org/10.1115/AJKFluids2019-5151.
[27] X.-X. Liang, N. Linz, S. Freidank, G. Paltauf, A. Vogel, Comprehensive analysis of spherical bubble oscillations and shock wave emission in laser-induced cavitation, J. Fluid Mech. 940 (2022), https://doi.org/10.1017/jfm.2022.202.
[28] R. Pecha, B. Gompf, Microimplosions: cavitation collapse and shock wave emission on a nanosecond time scale, Phys. Rev. Lett. 84 (2000) 1328–1330, https://doi.org/10.1103/PhysRevLett.84.1328.
[29] E. Faraggi, B.S. Gerstman, J. Sun, Biophysical effects of pulsed lasers in the retina and other tissues containing strongly absorbing particles: shockwave and explosive bubble generation, JBO 10 (2005), 064029, https://doi.org/10.1117/1.2139970.
[30] A.G. Doukas, A.D. Zweig, J.K. Frisoli, R. Birngruber, T.F. Deutsch, Non-invasive determination of shock wave pressure generated by optical breakdown, Appl. Phys. B Photophys. Laser Chem. 53 (1991) 237–245, https://doi.org/10.1007/BF00357143.

Žiga Lokar received B.Sc. and Ph.D. degree from the University of Ljubljana in 2011 and 2019, respectively. In 2018, he joined the Laboratory for Photonics and Laser Systems at Faculty of Mechanical Engineering, University of Ljubljana. His current research interests include study of light induced breakdown in water and other liquids, together with associated phenomena (shockwave, bubble, jetting).

Darja Horvat received both, the B.Sc. and M.Sc. degree in physics (1989 and 2000, respectively) from University of Ljubljana, Faculty of Mathematics and Physics and her PhD from University of Ljubljana, Faculty of Mechanical Engineering in 2004. She is with the University of Ljubljana, Faculty of Mechanical Engineering. Her research interests include laser ultrasonics and interaction of laser light with matter, mostly fluids.

Jaka Petelin was born in Ljubljana, Slovenia, in 1985. He received the B.S. and Ph.D. degree from the University of Ljubljana, Ljubljana, Slovenia in 2010 and 2015, respectively. From 2010–2016 he worked as a Senior Researcher at LPKF Laser & Electronics d.o.o. In 2016, he joined the Faculty of Mechanical Engineering, University of Ljubljana where he is working at the Laboratory for Photonics and Laser Systems. His research interests include development of new laser sources and their application for industry and medicine.

Rok Petkovšek was born in Ljubljana, Slovenia, in 1969. He received the B.S. and M.S. degrees in physics and the Ph.D. degree from the University of Ljubljana, Ljubljana, Slovenia in 1994, 1999, and 2003, respectively. From 1995–2003 he worked as a Researcher with the Jozef-Stefan-Institute. In 2003, he joined the Faculty of Mechanical Engineering, University of Ljubljana, as a Senior Researcher. There he founded a new Laboratory for Photonics and Laser Systems in 2016. He has served as its head ever since. Since 2016, he has also been the Chair of the Department of Optodynamics and Laser Technology, Faculty of Mechanical Engineering, University of Ljubljana. He has published more than 50 peer-reviewed journal articles. His research interests include development of new laser sources and their application for industry and medicine.